JOURNAL OF MATERIALS SCIENCE 13 (1978) 358–366

Effect of SiC content and orientation on the properties of Si/SiC ceramic composite

R. L. MEHAN
General Electric Company, Corporate Research and Development, Schenectady, New York 12301, USA

Silicon/silicon carbide ceramic composites are made by infiltrating carbonaceous material with liquid silicon to form SiC crystallites dispersed in a silicon matrix. The present study was conducted to determine the effects on the room temperature properties of density, elastic modulus, strength, and fracture toughness by varying the amount and distribution of the SiC crystallites. Most of the work involved uniaxially aligned SiC crystals of varying volume fraction tested both longitudinally and transversely to the converted fibre axis.

1. Introduction

Silcomp* is a family of Si/SiC ceramic composite materials developed recently at the General Electric Research and Development Center. The general properties of this material, as well as the fabrication method, have been previously described [1]. Briefly, the fabrication technique consists of infiltrating carbon fibres or fibrous material with liquid silicon at reduced pressure. The subsequent reaction between carbon and liquid silicon forms predominately β-SiC crystallites of sizes in the general range of 1 to 50 μm. The distribution of the starting carbonaceous material is preserved; that is, if the preform† consists of a block of uniaxially aligned carbon fibres, the final structure will consist of uniaxially aligned SiC crystallites in a silicon matrix. This is shown in Figs. 1 and 2, which are SEM photographs of such a structure after infiltration and with some silicon etched away to expose the converted fibres. The complexity of the resulting crystallites can be clearly seen in Fig. 2, which shows a variety of crystal sizes, shapes, and surface characteristics. By varying the amount, distribution and type of carbon in the preform, one can obtain a variety of structures. The flexibility of tailoring the structure as well as the ability to fabricate to final shape without

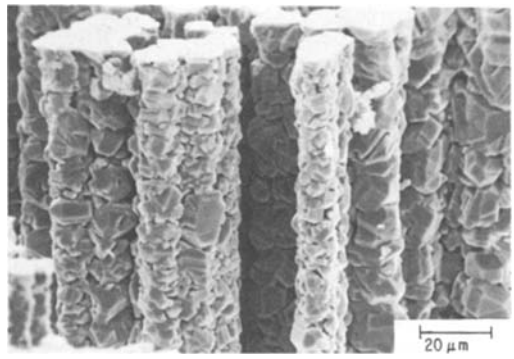

Figure 1 SEM photograph of longitudinally aligned SiC crystals. The silicon has been eteched away.

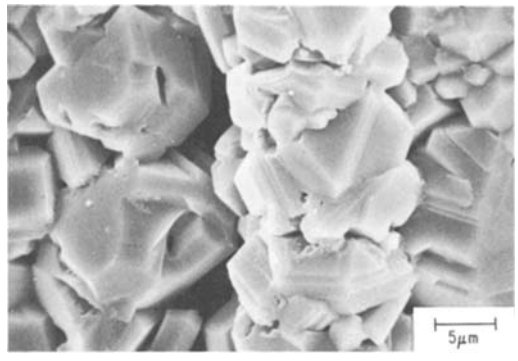

Figure 2 Same area as in Fig. 1 showing details of the converted SiC crystals.

*Trade mark.

†The term preform in the present context means the shaped piece of carbonaceous material, held together by a binder, prior to infiltration by silicon.

machining (the preform maintains its shape to ¼% after infiltration provided proper moulding procedure is used) are the features which make this material attractive. Prototype Si/SiC combustion liners have been run in turbine combustor test rigs [2], and more such work is planned for the future.

Previous publications have dealt with the anisotropic character of Si/SiC as affected by temperature [3] and the effect of temperature and time on the mechanical properties [4]. The present paper will deal with the effect on properties of the amount and distribution of converted SiC. Because silicon does exhibit plastic behaviour at temperatures above about 500° C [3], and it could be beneficial in some applications to utilize this fact to alleviate stress concentrations, it was considered of interest to gain some insight into the fracture behaviour of uniaxially aligned SiC crystals tested in both the longitudinal and transverse direction. Only room temperature properties will be considered here; the effect of temperature has been considered to some extent in the two previous publications and additional data will be published in the future.

2. Experimental

2.1. Procedure

The majority of the material prepared for this investigation consisted of carbon tow of varying amounts laid up into preform blocks about 3.5 cm wide, 5.5 cm long, and 1.0 cm thick. It was possible in this way to vary the volume fraction of SiC from 25% to about 80%. In all cases, 5 to 10% unreacted carbon is present in the infiltrated piece. The silicon used for infiltration was about 99% pure, containing Fe, Al, Cr, and Ca as major impurities. In some cases, carbon in the form of felt or cloth was used rather than tow. At present, most structural applications involving Si/SiC use carbon cloth to fabricate the preform.

Rectangular bend specimens either 0.25 or 0.51 cm square were removed from the infiltrated block both longitudinal and transverse to the original fibre direction. These were tested in three-point bending over two different span lengths; 1.71 and 3.81 cm, respectively. Although slightly different results should be obtained from these different specimen geometries because of the different stressed volumes, these differences are not considered significant. All tests were performed in an Instron testing machine at a rate of 0.013 cm min^{-1}.

Elastic modulus determinations were made using a sonic pulse echo technique. Volume fraction measurements were obtained by either standard point counting techniques or by estimation from typical microstructures. Fracture toughness values were mainly obtained with centre notched specimens 0.51 cm square with a 0.0305 cm wide notch 0.255 cm deep [5]. When a sharp crack was used, a technique similar to that used by Noone and Mehan [6] was employed. Specimens resembling a microscope slide, about 2.54 cm long and 0.80 mm wide, were first notched and then a sharp crack was induced by heating the base of the notch with a small oxy-hydrogen flame. The depth of this crack was measured, the specimen tested in three-point bending, and the fracture toughness was calculated from the relation [7]

$$K_{IC} = \frac{3}{2}\frac{P_f l}{bd^2}\sqrt{(\pi c)}F(c/d) \quad (1)$$

where P_f = fracture load, l = testing span, b, d = specimen width and height, respectively, c = crack depth (notch and thermal crack), $F(c/d)$ = geometric constant depending on the span length and crack-to-height ratio (tabulated in Reference [7]).

2.2. Microstructures

Typical transverse microstructures containing low (~25 vol %), medium (~60%), and high (~80%) SiC volume fractions are shown in Figs. 3, 4 and 5. A longitudinal section of a medium volume fraction specimen is shown in Fig. 6, where the aligned nature of the SiC is evident. The original distribution of the carbon fibre bundles are clearly shown in Figs. 3 and 4. It was not found possible to spread the fibres in the preform to any greater

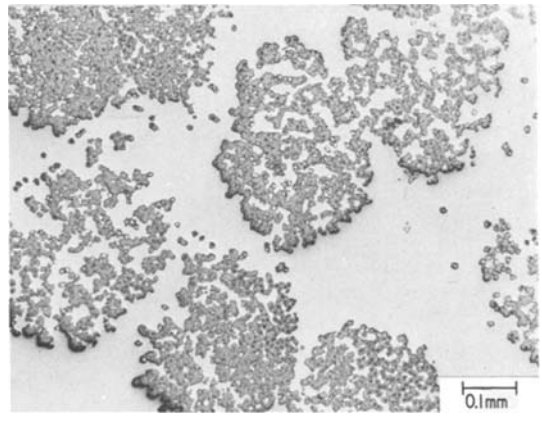

Figure 3 Transverse section of a specimen containing a low SiC volume fraction.

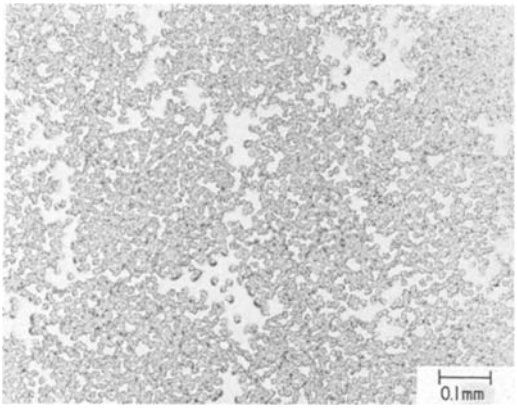

Figure 4 Transverse section of a specimen containing a medium SiC volume fraction.

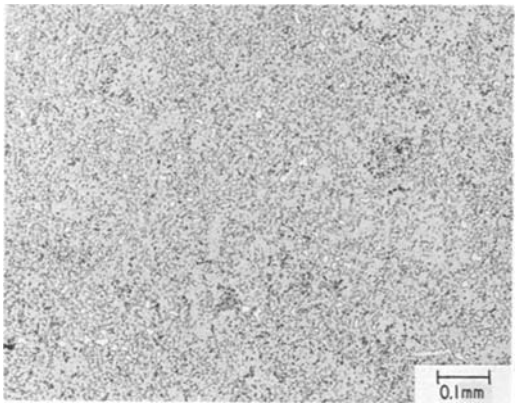

Figure 5 Transverse section of a specimen containing a high SiC volume fraction.

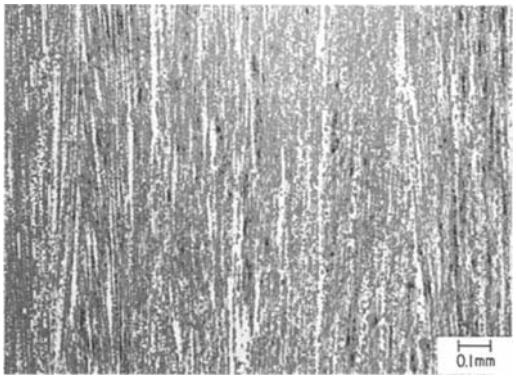

Figure 6 Longitudinal section of a specimen containing a medium SiC volume fraction.

extent than that depicted in Fig. 3. Consequently, in the low volume fraction region using tow material, the converted fibres distribution is clustered.

It may be pointed out that the silicon grain size

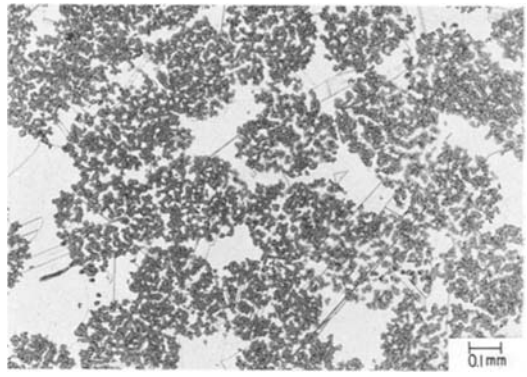

Figure 7 Transverse section of a Si/SiC composite with the silicon etched. Note large grain size and finer microstructural features.

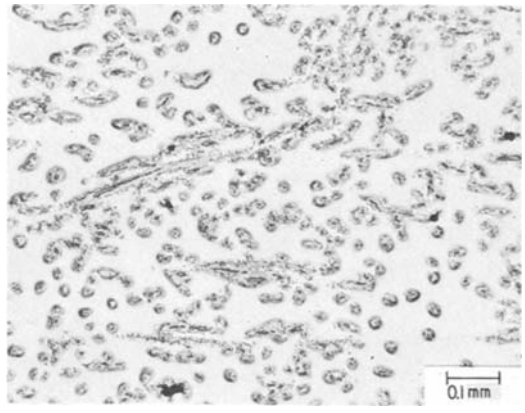

Figure 8 Microstructure of Si/SiC using carbon felt as the precursor material.

is quite large. This is shown in Fig. 7 for a fairly low volume fraction specimen. As may be seen, the average grain size is far larger than the fibre bundles, but microstructural features resembling twins occur on a finer scale. As will be discussed later, these features play a role as the strength controlling defect in Si/SiC tested transverse to the "fibre" direction.

The microstructure of Si/SiC derived from carbon felt is shown in Fig. 8. This material, because of the fairly uniform dispersion of the SiC particles, would be expected to behave in an isotropic manner, as distinct from the tow derived material. The mechanism of SiC crystallite formation, however, remains the same. This may be seen in the SEM photograph shown in Fig. 9, where the silicon has again been etched away to reveal the converted carbon. The crystallite size tends to be somewhat smaller than those shown in Figs. 1 and 2, with sizes present of about 20 to 30 μm and

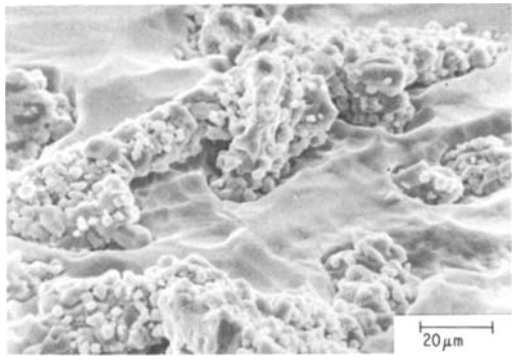

Figure 9 SEM photograph with silicon etched away of a felt derived structure showing the SiC crystal size.

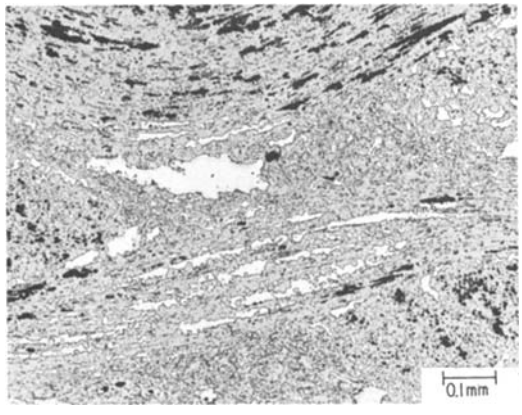

Figure 10 Microstructure of Si/SiC using carbon cloth as the precursor material.

smaller. This may be related to the more amorphous character of the felt, but the exact reason cannot be positively identified. Finally, Fig. 10 depicts the microstructure associated with material made from carbon cloth. The cross-ply characteristics of this material are evident, and its properties are isotropic in the plane of the cloth.

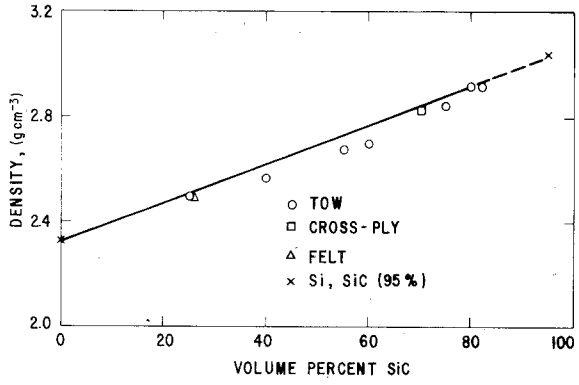

Figure 11 Density as a function of SiC volume fraction for three Si/SiC structures.

3. Results

The property data obtained on the Si/SiC structures described in Section 2.2 are shown in Figs. 11 to 14. In most cases, density and moduli values represent the average of two specimens; strength and fracture toughness values between three and five. Where appropriate (three or more values), the standard deviation of the results are shown. The values for pure silicon are for pre-cleaved silicon single crystals from recent work by St. John [8].

4. Discussion

4.1. Density

The density of multiphase materials should follow the "rule of mixtures" quite well, and the data in Fig. 11 illustrate this point. Deviations from the straight line represent either error in density measurement (obtained either by immersion methods or by weight and dimensional measurements) or the presence of an excessive amount of

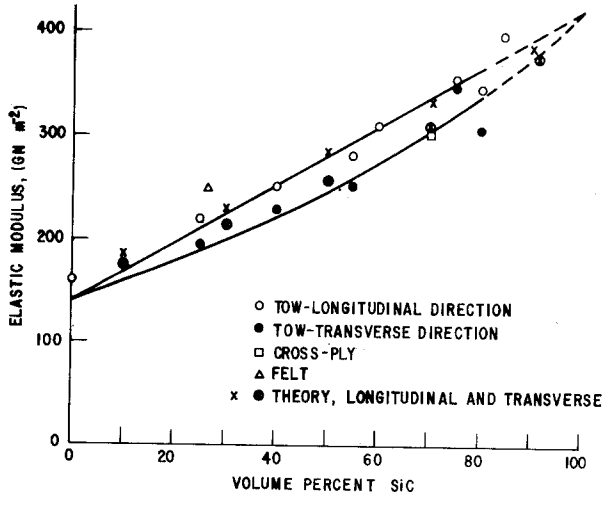

Figure 12 Experimental and theoretical elastic modulus as a function of SiC volume fraction for three Si/SiC structures.

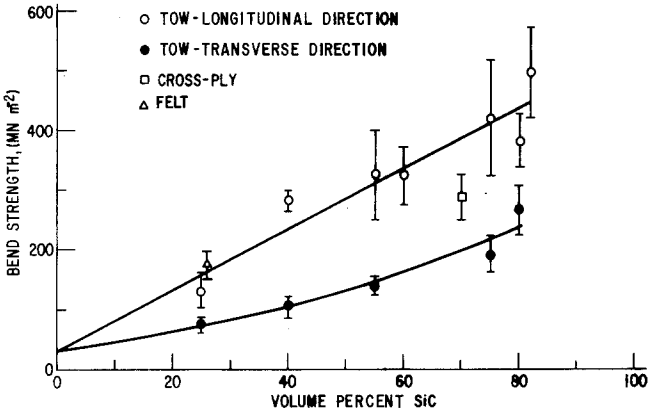

Figure 13 Strength as a function of SiC volume fraction for three Si/SiC structures. Bars indicate the standard deviation.

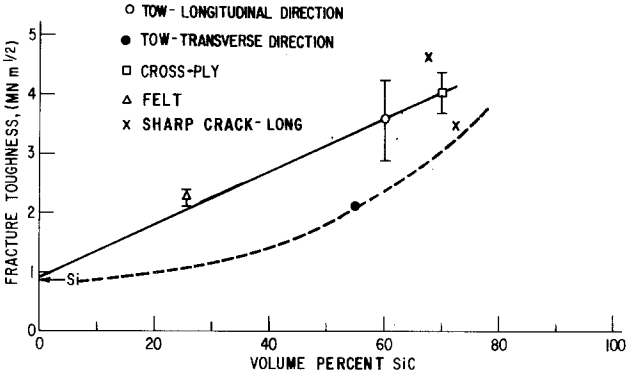

Figure 14 Fracture toughness as a function of SiC volume fraction for three Si/SiC structures and machined notches (open points) and a sharp crack. Bars indicate the standard deviation.

unreacted carbon. There is always at least 5% unreacted carbon present (hence the use of 95% dense SiC as the end point), but at times more can be present; this can be seen by referring to Fig. 10. In any event, the experimental points fall on a straight line joining the density of pure silicon ($2.33\,g\,cm^{-3}$) and 95% dense SiC ($3.04\,g\,cm^{-3}$) within 3%.

4.2. Elastic modulus

The values for material fabricated from carbon tow and tested in the longitudinal direction follow a linear dependence upon volume fraction, as expected for a uniaxially aligned reinforcement [9]. For these data (open circles in Fig. 12), a least squares line was fitted to the data, using values of $161\,GN\,m^{-2}$ and $410\,GN\,m^{-2}$ for silicon [10] and 95% dense SiC [11]. The silicon data in Reference [10] are given in terms of the elastic stiffness, C_{11}, C_{12}, and C_{44}. These were converted to elastic compliance (S_{ij}), and the modulus for a random orientation computed from the relation given by Date and Andrews [12]. The curve for moduli in the transverse direction was estimated, using the self-evident fact that at 0 and 95% SiC (5% carbon/porosity assumed) the longitudinal and transverse values are identical*.

The theoretical values shown in Fig. 12 were computed from the Halpin–Tsai equations [9]. These are

$$E_{11} \simeq E_r V_r + E_m(1 - V_r) \quad (2)$$

$$E_{22} = E_m \frac{1 + \xi\eta V_r}{1 - \eta V_r} \quad (3)$$

where E_{11} = modulus in the longitudinal direction, E_{22} = modulus in the transverse direction, E_r = modulus of the reinforcing phase ($410\,GN\,m^{-2}$ in the present case), E_m = modulus of the matrix phase ($161\,GN\,m^{-2}$ in the present case), V_r = volume fraction of the reinforcing phase, ξ = shape factor; in the present case given as $\xi = 2(a/b)$ where a and b are the width and thickness of the reinforcing crystal. These are assumed equal so that $\xi = 2$, $\eta = (E_r/E_m - 1)/(E_r/E_m + \xi)$. The

*There are, of course, more than two elastic constants involved for such an anisotropic material as Si/SiC. In the general case, for an orthotropic material with three mutually perpendicular planes of symmetry, there are nine independent elastic constants.

theoretical values shown in Fig. 12 have the correct form but are displaced from the experimental results at the lower volume fractions. This is because the least-squares line extrapolated to a value of $E_m = 140\,GN\,m^{-2}$, rather than the value used in the above equations ($161\,GN\,m^{-2}$). The reason for the felt-derived material (open triangle) having such a high modulus, considering the density fell on the "rule of mixtures" line, is not known.

4.3. Strength and Fracture Toughness

As in the case of the elastic modulus, the strength of the tow-derived material (Fig. 13) tested in the longitudinal direction increases linearly with SiC content; again a least-squares line was fitted to the data. The curve for the transverse direction was estimated. As might be expected, the crossply material (open square) falls between the upper and lower bounds of strength. However, the felt-derived material should also be between these bounds because of its isotropic nature. As in the case of the elastic modulus, its strength value seems somewhat higher than one would expect.

Fracture toughness increases with SiC content within the volume fraction range studied. For this material, machined notches and sharp cracks give the same values of toughness, based on somewhat limited data. This is in contrast to a similar material, self-bonded SiC (Refel* SiC) [13]. In Refel, it was found that the room temperature fracture surface energy was overestimated by about 50% by employing machined notches versus sharp cracks.

When attempting to rationalize the strength and toughness behaviour of Si/SiC as affected by volume fraction, one is faced with a dilemma. On the one hand, there is a large body of literature regarding ductile matrices reinforced with both continuous and discontinuous filaments. Much of this information has been recently summarized [14]. On the other, the strength behaviour of two-phase ceramics, with the second phase distributed as discrete particles, is also reasonably well understood [15–17]. There is also information available on brittle fibres dispersed in a brittle matrix [18, 19]. The strengthening mechanism of dense, highly packed SiC crystals in an Si matrix is also understood [13]; this latter strengthening mechanism should apply to isotropic Si/SiC (or Si/SiC tested in the longitudinal directions) above about 85% SiC content. Here the microstructures of self-bonded SiC and Si/SiC are virtually identical and their properties similar. However, at lower volume fractions where anisotropy is present, the present Si/SiC system, consisting of semi-continuous and aligned crystals of SiC distributed in a brittle matrix, falls between the extremes given by composite and ceramic experience. In some cases, as in the prediction of some of the elastic constants, composite theory applies. However, in the case of the strength data shown in Fig. 13, a significant difference exists between conventional composite theory and the transverse strength of Si/SiC. In the case of a ductile metal reinforced with a brittle fibre and tested in the transverse direction, the strength either rises slightly, but more generally remains the same or decreases with increasing filament volume fraction [20]. In the present case (Fig. 13), the transverse strength rises continuously with increasing volume fraction, indicating a different strengthening mechanism.

No attempt will be made here to develop a rigorous strengthening theory for anisotropic Si/SiC. For one thing, the data base is deficient (testing at various angles to the original fibre axis, for example, and more fracture toughness data in the transverse direction). Nevertheless, several observations can be made concerning the data which may be of interest.

4.3.1. Strength in the longitudinal direction

It is possible to consider the aligned SiC crystallites to consist of an *in situ* composite filament. This is not entirely unreasonable, as it is known the SiC–SiC bonds do possess some strength because a cross-ply composite retained a strength of about $83\,MN\,m^{-2}$ to temperatures of 1600° C where the silicon is completely molten [4]. Assuming a room temperature matrix strength of $44.8\,MN\,m^{-2}$, the "filament" strength can be calculated from

$$\sigma_c = \sigma_f V_f + \sigma_m(1 - V_f) \qquad (4)$$

where σ_c = composite strength, σ_f = "filament" strength, σ_m = matrix strength ($44.8\,MN\,m^{-2}$), V_f = volume fraction "filaments". When σ_f is computed in this way, it has an average strength of $541\,MN\,m^{-2}$. A comparison of observed versus calculated strengths based on this value are shown in Table I. Perhaps the best use of this approach lies in estimating a reasonable upper strength level for Si/SiC using current fabrication methods,

*Trade mark.

TABLE I

Volume fraction of "filaments"	Observed strength ($MN\,m^{-2}$)*	Calculated strength ($MN\,m^{-2}$)
0.2	145	144
0.4	241	243
0.6	345	343
0.8	441	442
1.0	–	541

which is of the order of $541\,MN\,m^{-2}$. Other than this estimate, it cannot predict transverse properties and offers no insight into the fracture mechanism.

A more fruitful approach lies in making use of Equation 1 and the fracture energies shown in Fig. 14*. All the longitudinal specimens (except for the ones containing a sharp crack) were 5.08 mm square, were tested over a 3.81 cm span, and were notched half-way through; $F(c/d) = 1.47$ for this case. Using Equation 1 and the modulus and strength data in Figs. 12 and 13, the corresponding critical flaw size can be calculated. This is shown in Table II. The felt-based material is shown separately because it was indicated earlier that the SiC crystallite size seemed smaller. The calculated value, however, seems larger than the tow derived material. No explanation is immediately evident.

TABLE II

Volume fraction	Calculated critical flaw size (μm)
0.2	41
0.4	30
0.6	26
0.8	23
0.26 (Felt)	45

Thc systematic decrease of the calculated flaw size is not entirely understood. It is difficult to etch away silicon and observe individual crystals in the higher volume fraction composites, and it is possible the average size is smaller. It is also possible that, at lower volume fractions, machined notches overestimate the fracture toughness somewhat, thus leading to somewhat lower calculated flaw sizes. Nevertheless, the calculated flaw size, which is in the range of 20 to 45 μm, is of the same order of size as the larger of the converted SiC crystallites, which makes it likely this is the strength controlling structural feature. It is of interest to note that flaw depths of the same order of size, 15 to 70 μm, have been calculated for self-bonded SiC [13].

4.3.2. Strength in the transverse direction

Data are even scarcer here than in the longitudinal direction. Only one K_{IC} measurement could be conducted because of specimen size limitations, and this was done with a machined notch†. The dotted curve has been fitted through this point, the pure Si point, and the assumption that the transverse properties will approach the longitudinal properties as the volume fraction increases and the SiC crystals become interconnected both in the axial and transverse direction. With the full knowledge that the fracture toughness data are on very shaky ground, it is of interest to again compute the critical flaw size from Equation 1. At least one point should be correct, assuming the same equivalence between machined and sharp cracks observed in the longitudinal direction. These data are shown in Table III.

TABLE III

Volume fraction	Calculated critical flaw size (μm)
0	98
0.2	74
0.4	76
0.6	112

If the estimated curve in Fig. 14 is approximately right, it would indicate that for toughness in the transverse direction, the critical flaw remains about constant and equal to the microstructural features giving rise to the fracture in the pure silicon; i.e., those shown in Fig. 7. This seems reasonable for volume fractions up to about 60% SiC, as the individual fibre bundles still show separation of at least this distance. Above about 60%, however, the crystals tend to be interconnected both axially and transversely, and the critical flaw size would be expected to approach that discussed in the previous section.

*The use of such an equation derived for the case of isotropic material for an anisotropic one has been shown to be valid if the crack is perpendicular to one of the three axis of symmetry [21].

†It is possible to produce a notch in a transversely oriented specimen in one of two ways. In both the notch is parallel to the aligned crystallites, but in viewing the transverse section one sees the notch parallel to the aligned crystals in one case and the notch extending into the "fibre" bundles (as seen end-on) in the other. Kreider [22] refers to this as orientation 2 and 3, respectively, in boron-reinforced aluminium, and finds little difference in impact properties between them. It is assumed no difference exists in these two orientations in Si/SiC, but this has not been experimentally verified.

It may be pointed out that other explanations to account for the transverse strength were seriously considered. In particular, the theory advanced by Hasselman and Fulrath [16] seemed an attractive explanation for the transverse strength behaviour. Their method involves the use of the Griffith equation, using the fracture surface energy and modulus of the matrix and the inter-particle spacing as the flaw size. Their numerical predictions, however, did not correspond to the experimental results. This could be due to the large distribution of particle spacings, and the fact the particles are a continuous array of crystals. Theories involving thermomechanically induced strengthening mechanisms, such as that recently proposed by Borom [23], are not applicable because of the close match of the thermal expansion coefficient of Si and SiC.

4.3.3. Cross-ply material

There are insufficient data to draw any conclusions on the cross-ply data, except to observe the strength lies between the upper and lower bounds and the fracture toughness lies on the curve applicable to the longitudinal data. The latter observation is not unreasonable; a crack moving through a cross-ply structure will encounter fully as many obstacles to its movement as in the case of a crack moving perpendicular to the aligned crystallites. This is shown in Fig. 15, taken from reference [4], which shows a crack introduced in a bend test above the silicon melting point, arrested, allowed to cool so the crack was filled with silicon at room temperature. The tortuous path of the crack is evident. It may be noted the calculated critical flaw size for this material is of the order of 62 μm; this may reflect the presence of the occasional islands of silicon shown in Fig. 10.

5. Conclusions

From the results of this study, the following conclusions may be drawn:

(1) The strength of Si/SiC fabricated using carbon tow as the carbon precursor and tested longitudinally to the converted fibre direction increased in a linear manner to a maximum value of 501 MN m^{-2} at 82 vol % SiC. At these volume fractions, the material has properties somewhat

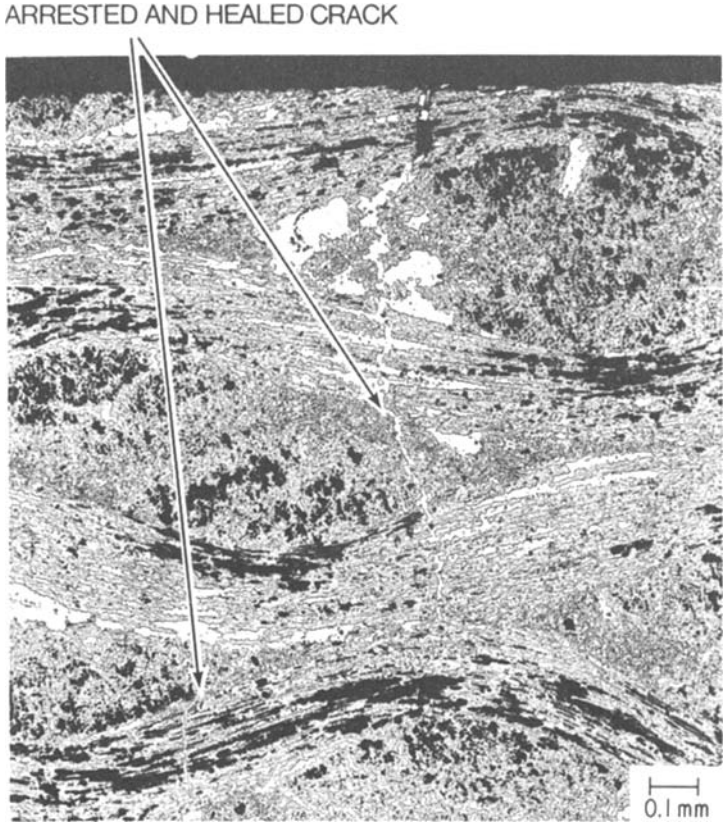

Figure 15 Photograph of an arrested and healed crack in cloth derived Si/SiC showing the erratic fracture path.

similar to self-bonded SiC and throughout the volume fraction range (25 to 82 vol % SiC) has a calculated critical flaw size in the range 23 to 45 μm, which corresponds to the size of the converted SiC crystallites.

(2) The same material tested transversely to the converted fibre direction is much weaker and has a non-linear dependence of strength on volume fraction and increases more rapidly at higher values. This is attributed to interconnectivity of the transformed crystals in both the axial and transverse direction.

(3) The strength controlling defects in the transverse direction at lower volume fractions seem to be related to microstructural features, perhaps twins, in the silicon matrix.

(4) Material fabricated from cross-plied carbon cloth has properties intermediate between the longitudinal and transverse case.

Acknowledgments

The author would like to acknowledge the assistance of W. Laskow for fabricating the Si/SiC material and W.S. Coblenz for performing some of the testing. The metallographic work is primarily due to B. Beach and J. Methé. I am indebted to both C.R. Morelock and W.B. Hillig for discussions concerning the behaviour of this sometimes perplexing material.

References

1. W. B. HILLIG *et al. Amer. Ceram. Soc. Bull.* **54** (1975) 1054.
2. C. M. GRONDAHL and B. W. GERHOLD, *Amer. Soc. Mech. Engr.*, Paper 76-GT-22 (1976).
3. R. L. MEHAN, *Amer. Ceram. Soc. Bull.* **56** (1977) 211.
4. G. G. TRANTINA and R. L. MEHAN, *J. Amer. Ceram. Soc.* **60** (1977) 177.
5. R. W. DAVIDGE and A. G. EVANS, *Mat. Sci. Eng.* **6** (1970) 281.
6. M. J. NOONE and R. L. MEHAN, "Fracture Mechanisms of Ceramics, Vol. I" (Plenum, New York, 1973) p. 201.
7. H. TADA, "The Stress Analysis of Cracks Handbook" (Del Research Corp., Hellertown, Pennsylvania, 1973) p. 2.16.
8. C. St. JOHN, *Phil. Mag.* **32** (1975) 1193.
9. J. E. ASHTON *et al.*, "Primer on Composite Materials" (Technomic, Stamford, Conn., 1969) p.77.
10. W. R. RUNYAN, "Silicon Semiconductor Technology" (McGraw–Hill, New York, 1965) p. 213.
11. W. S. COBLENZ, *J. Amer. Ceram. Soc.* **58** (1975) 530.
12. E. H. F. DATE and K. W. ANDREWS, *Brit. J. Appl. Phys.* **2** (1969) 1373.
13. J. R. McCARREN *et al. Proc. Brit. Ceram. Soc.* **20** (1972) 259.
14. K. G. KREIDER, "Metallic Matrix Composites" (Academic Press, New York, 1974).
15. R. W. DAVIDGE, T. J. GREEN, *J. Mater. Sci.* **3** (1968) 629.
16. R. M. FULRATH and J. A. PASK, "Ceramic Microstructures" (John Wiley, New York, 1968) p. 343.
17. H. LIEBOWITZ, "Fracture, Vol. VII" (Academic Press, New York, 1972) p. 729.
18. A. W. HOLDSWORTH and M. J. OWEN, *J. Comp. Mat.* **8** (1974) 117.
19. D. C. PHILLIPS, *et al. J. Mater. Sci.* **7** (1972) 1454.
20. K. G. KREIDER, "Metallic Matrix Composites" (Academic Press, New York, 1974) p. 445.
21. G. C. SIH, P. C. PARIS and G. R. IRWIN, *Int. J. Fract. Mech.* **1** (1965) 189.
22. K. G. KREIDER, "Metallic Matrix Composites" (Academic Press, New York, 1974) p. 455.
23. M. P. BOROM, *J. Amer. Ceram. Soc.* **60** (1977) 17.

Received 29 April and accepted 30 May 1977.